

High throughput measurements of soft x-ray impurity emission using a multilayer mirror telescope

D. Stutman, K. Tritz, L. Delgado-Aparicio, and M. Finkenthal
Johns Hopkins University, Baltimore, Maryland 21218

G. Suliman
National Institute of Physics and Nuclear Engineering, Bucharest, R-76900 Romania

L. Roquemore, R. Kaita, H. Kugel, and D. Johnson
Princeton University, Princeton, New Jersey 08543

N. Tamura, K. Sato, and S. Sudo
National Institute for Fusion Science, Toki 509-5292, Japan

C. Tarrio
National Institute of Standards and Technology, Gaithersburg, Maryland 20899

(Received 8 May 2006; presented on 10 May 2006; accepted 12 June 2006; published online 17 October 2006)

A 4 in. multilayer mirror telescope has been tested on National Spherical Torus Experiment (NSTX) for high throughput measurements of the beam excited soft x-ray impurity emission. The design is aimed at imaging low- k turbulent fluctuations in the plasma core. The test device used curved and planar Mo/Si mirrors to focus with $\approx 15\%$ optical transmission and few angstrom bandwidths, the 135 \AA Ly $_{\alpha}$ line from injected Li III atoms, or the $n=2-4$ line from intrinsic C VI ions. As test detectors we used 1 cm^2 absolute extreme ultraviolet diodes, equipped with 400 kHz bandwidth, low noise preamplifiers. With the available view on NSTX the telescope successfully detected small impurity density fluctuations associated with 1/1 modes rotating at midradius, indicating that a high signal to noise ratio and cost effective core turbulence diagnostic is feasible based on this concept. © 2006 American Institute of Physics. [DOI: [10.1063/1.2227436](https://doi.org/10.1063/1.2227436)]

I. INTRODUCTION

One of the most successful techniques for the study of low- k fluctuations in the core of tokamak plasmas is the beam emission spectroscopy (BES).¹ Unique insight into the tokamak turbulence has been obtained by fast imaging of centimeter sized, radial and poloidal fluctuations in the D $_{\alpha}$ light emitted by neutral beams.² The diagnostic we study is also a beam based imaging system, with one fundamental difference, however. Instead of the beam D $_{\alpha}$ emission, it will use for turbulence imaging one of the bright soft x-ray lines of low- Z impurities, excited by charge exchange (CX) with the neutral beams. Fluctuations in this emission reflect impurity density fluctuations, which are similar to the electron density fluctuations measured by conventional BES. In this approach, the visible light focusing lenses, optical fibers, and spectrometers of conventional BES are replaced by a focusing multilayer mirror (MLM) telescope, which collects, images, and spectrally filters the beam excited impurity light within a single optical system.³ The impurities can be either intrinsic, such as carbon or lithium from the plasma facing components, or injected in diagnostic pellets such as tracer embedded solid pellet (TESPEL) (Refs. 4 and 5 and references therein).

In comparison with the conventional BES technique, the soft x-ray telescope can have important advantages.³ First, the CX excited soft x-ray lines of low- Z impurities are much

brighter than the beam D $_{\alpha}$ emission and also much more energetic. This is illustrated in Fig. 1 by a plot of the C VI H $_{\alpha}$ ($n=2-3, \lambda \approx 182 \text{ \AA}$) emitted power as a function of major radius, estimated for a typical H-mode plasma in the National Spherical Torus Experiment (NSTX), using the computed beam density for 90 kV beams and assuming a 30 cm line of sight through the beam. We used the effective CX rate coefficients from Ref. 6, which include collisional mixing effects. A uniform C density of 10^{12} cm^{-3} ($\approx 2\%$ of the central electron density) was assumed. For comparison, the estimated deuterium D $_{\alpha}$ power is also shown. As seen, the power emitted in the beam excited C VI H $_{\alpha}$ line is about 20 times higher than that in the beam D $_{\alpha}$ emission. In addition, the low- Z impurity density can, in principle, be increased up to several percent, by external seeding of the plasma.

Another advantage of the multilayer mirror telescope is that it combines in a single instrument the collecting and imaging optics and the wavelength filtering spectrometer, thus enabling simple and high throughput systems for two dimensional (2D) imaging of fluctuations.³ This aspect was also discussed in the context of imaging the deuterium Ly $_{\alpha}$ beam emission at 1216 \AA with vuv multilayer mirrors.⁷ Considering also the high power available in the CX excited soft x-ray lines, the proposed telescope can thus considerably simplify and reduce the cost of low noise and fast detection systems needed for turbulence imaging.

However, these advantages come together with one

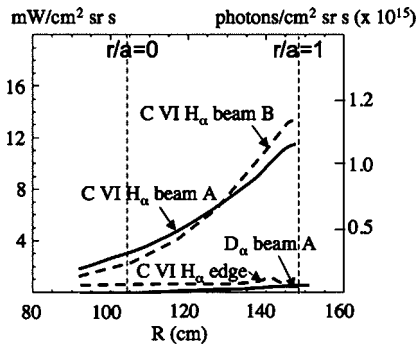


FIG. 1. Computed power and brightness of the beam excited C VI H_{α} transition ($\lambda \approx 182 \text{ \AA}$) as a function of major radius, for 2% C concentration and typical NSTX H -mode profiles. The beams have 90 keV energy and tangency radii of 70 cm (A) and 60 cm (B). The brightness is computed assuming a 30 cm integration path through the beam. The power estimated for the D_{α} emission from beam A and the brightness of the C VI H_{α} emission from the plasma edge (dotted line) are also shown.

drawback. While separating very well the line of interest from the overall plasma spectrum, the multilayer mirrors in the telescope do not have sufficient spectral resolution to discriminate between the beam core emission and the background edge emission at the same wavelength. However, as illustrated also in Fig. 1 by a computation of the C VI H_{α} brightness from the H -mode edge, this emission can be expected to be much less intense than that excited by the beam. The photon noise from the background at 135 \AA will therefore not affect much the useful signal, allowing one to perform cross-correlated measurements of the core fluctuations. Lastly, the mirrors reflect also background light from the visible to the vuv, which can be suppressed by a thin foil filter passing radiation below 200 \AA approximately.

A prototype telescope for the 135 \AA wavelength and aimed at measuring the Ly_{α} transition emitted by injected Li III atoms, or the $n=2-4$ transition from intrinsic C VI ions, has been built and tested on NSTX, as described in the following.

II. PROTOTYPE 135 \AA TELESCOPE ON NSTX

The conceptual design of multilayer mirror based telescopes for fluctuation imaging has been discussed in Ref. 3. At wavelengths above $\approx 100 \text{ \AA}$, using near normal incidence mirrors enables designing low f -number systems having very high optical throughput. This is because at normal incidence the width of the Bragg peak is large, enabling rays in a broad angular range to be reflected with near maximal reflectivity.

The optical layout of the test NSTX device is shown in Fig. 2(a). A planar Mo/Si multilayer mirror of 4 in. diameter deflects and prefilters the incoming light, while a second spherical ($R=1.0 \text{ m}$) mirror, also of 4 in. diameter and operated near normal incidence ($\theta_B=85^\circ$), focuses the 135 \AA light towards the detectors. The spherical mirror has multilayer period $2d \approx 138 \text{ \AA}$, $N=50$ layers and $\Gamma=d_{\text{Mo}}/2d \approx 0.4$, while the planar mirror has $2d \approx 200 \text{ \AA}$ and the same number of layers and Γ as the spherical one. Both mirrors were manufactured by the NTT Advanced Technology Corp., Japan.⁸ The reflectivity and spectral band pass of the mirrors have been calibrated using synchrotron light at NIST, as well

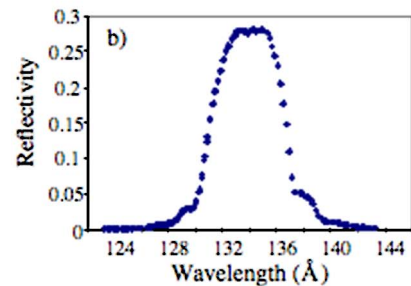
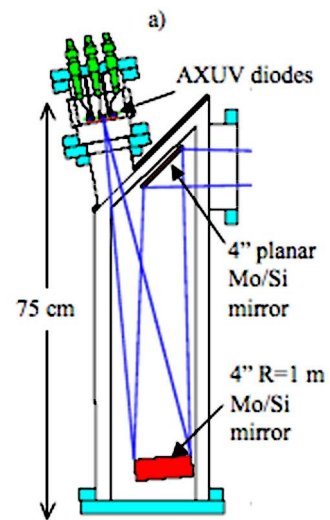


FIG. 2. (Color online) (a) Layout of the 135 \AA prototype telescope. (b) Overall reflectivity and spectral band pass of the telescope multilayer mirror system.

as using an electron impact laboratory source, based on the 135 \AA Si L -shell emission. The reflectivity of the compound mirror system is shown in Fig. 2(b). A filter composed of $0.3 \mu\text{m}$ Be on $0.1 \mu\text{m}$ Parylene-N and manufactured by Lebow Corp.⁹ is used to block the visible to vuv background light. Including the attenuation of this filter the overall optical transmission of the system is thus around 15%, while the spectral band pass is only a few angstroms.

Since the primary goal of the NSTX measurements was to verify the signal-to-noise ratio (SNR) and light gathering capability of the telescope, as test detectors we used 1 cm^2 area, AXUV SP-2 diodes manufactured by International Radiation Detectors Inc., USA, which have nearly 100% quantum efficiency at the wavelengths of interest.¹⁰ With about 60% of the diode area exposed to plasma light, a large geometrical throughput of $\approx 10^{-2} \text{ cm}^2 \text{ sr}$ was achieved. The diode currents were amplified with using low noise, 10^7 V/A gain, and 400 kHz bandwidth preamplifiers, custom developed for use with large area AXUV diodes by Accent Pro 2000, Romania.¹¹ An important feature of these preamplifiers is that they maintain their low noise and large bandwidth, even when used with high capacitance detectors, or long connecting cables.

The view available on NSTX for our tests is shown in Fig. 3. The central detector of the instrument was focused in the footprint of beam B at $R \approx 65 \text{ cm}$, with a demagnification around six. This radius corresponds to a normalized flux coordinate $r/a \approx 0.4-0.5$, but on the *inboard* side of the

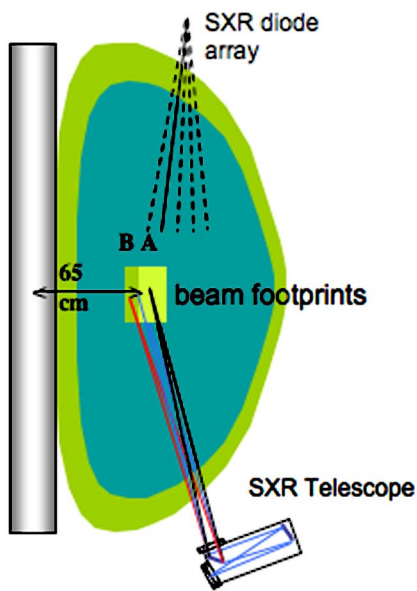


FIG. 3. (Color online) View of the prototype 135 \AA telescope for the tests on NSTX. The chords of the vertical SXR diode array are also indicated.

magnetic axis. In this view, perpendicular to the field lines and having several centimeter toroidal and radial extents, the telescope can detect only larger scale magneto-hydrodynamic (MHD) perturbations. In addition, at this in-board location the beam has traveled a long path through the plasma and is strongly attenuated, especially in H modes (Fig. 1). Finally, at this location, in addition to the beam volume the instrument viewed also the plasma around the upper divertor, a region of intense line emission.

Most instrumental tests were performed using the $n=2-4$, 135 \AA transition of intrinsic C VI, excited by charge exchange with the beam in the plasma center and by collisional excitation and recombination in the edge and divertor regions. The NSTX spectrum around 135 \AA was previously measured using a photometrically calibrated grazing incidence spectrometer, having a similar plasma view as the telescope in Fig. 3. The spectrum is dominated by the C VI 135 \AA line, with a typical brightness of a few 10^{13} photon/cm² sr s in low density L modes.

The signal from the innermost viewing telescope detector, obtained during a low density L -mode discharge heated by beam A at 90 kV and 2 MW power, is shown in the left panel of Fig. 4(a). In these L -mode plasmas the carbon profile measured by charge exchange recombination spectroscopy is strongly peaked, thus enhancing the contribution from the beam excited emission in the core over the edge and divertor emission. In these conditions, the telescope successfully detects the small carbon density fluctuation associated with a 1/1 MHD perturbation at midradius. This is shown in Figs. 4(b) and 4(c) by the comparison between the telescope fluctuations and those from a soft x-ray diode filtered for the high energy core emission (right panels). The filtered soft x-ray diode viewed the plasma along a vertical chord crossing the midplane at about the same radius where the innermost telescope diode is focused. The near identity of the Fourier spectrograms clearly shows that the telescope can

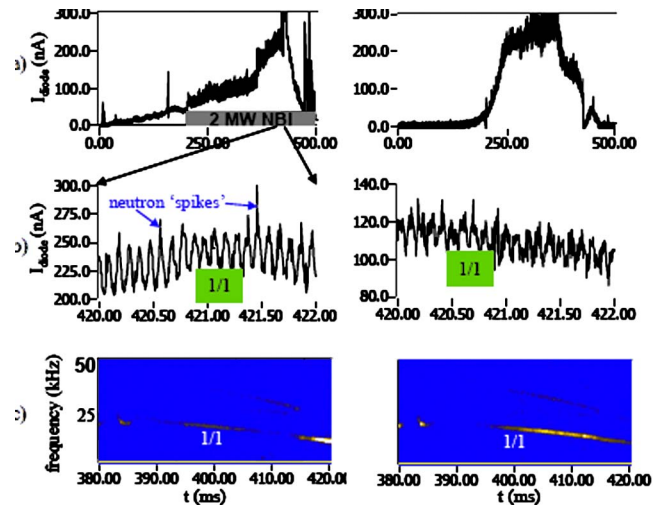


FIG. 4. (Color online) Signal from the telescope diode viewing beam A in low density L -mode discharge, sampled at 190 kHz (left panels). For comparison, in the right panels is shown the signal from the chord at $R \approx 68$ cm of the vertical SXR diode array on NSTX ($E > 1.4$ keV core emission). (a) Time history of the telescope and SXR signals during the discharge. (b) Expanded traces during the onset of a 1/1 MHD mode, located around midradius. (c) Fourier spectrograms of the telescope and core SXR fluctuations.

image localized fluctuations in the beam excited emission from the plasma center. Figure 4(b) shows also that a high SNR can be achieved with this instrument. Finally, concerning the intensity of the emission, the signal level in Fig. 4(a) corresponds to a few 10^{13} photon/cm² sr s in the 135 \AA line, consistent with the brightness previously measured by the soft x-ray (SXR) spectrometer.

In addition, Figs. 4(a) and 4(b) indicate that the main source of high frequency noise in the telescope signals are the “spikes” arising from energetic neutrons and gamma rays interacting in the AXUV diode. As seen in the expanded trace in Fig. 4(b), however, these spikes are rather infrequent and also very sharp, typically covering one sample time.

The picture of the telescope signals changes in high density H modes, where the carbon profile is very hollow, and the beam attenuation at $R < 70$ cm is much stronger (Fig. 1) than in L modes. In these conditions, the telescope measures predominantly the 135 \AA emission from the pedestal and divertor region. The typical trace is shown in Fig. 5(a) and exhibits the characteristic bursts of type I edge localized modes (ELMs). The expanded view in Fig. 5(b) and the frequency spectra show, however, only low frequency (<several kilohertz) noise, together with neutron spikes. The intensity of the 135 \AA edge emission is also low in H modes, with brightness of the order of 10^{13} photons/cm² sr s.

Finally, within experiments aimed at studying perturbative electron transport, we injected both conventional Li pellets and Li tracer TESPEL pellets in several H - and L -mode NSTX discharges. A strong burst of Li III Ly $_{\alpha}$ emission is observed in the telescope signal following injection of 0.5 mg (5×10^{19} atoms) conventional Li pellets into high power and density H modes, at injection velocity around 100 m/s. Fast imaging with visible light cameras filtered for Li I emission indicates that although a substantial T_e perturbation is produced, the pellet penetrates only to the plasma

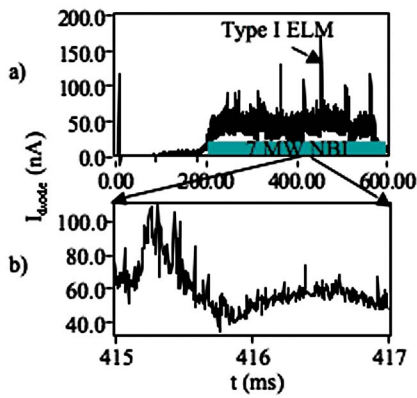


FIG. 5. (Color online) (a) Telescope signal in high density and power H mode, showing type I ELMs. (b) Expanded view showing only low frequency fluctuations from peripheral MHD and neutron spikes.

edge. In low density L modes on the other hand, the pellet penetrates to $r/a \approx 0.6$, giving rise to a large telescope signal ($\leq 10^{15}$ photon/cm² sr s). The first data from injection of C₈D₈ TESPEL shells loaded with $\approx 4 \times 10^{17}$ Li atoms indicate shallower penetration than with conventional pellets (few cm inside the separatrix of low density L modes), but much more localized Li deposition [Fig. 6(a)]. The telescope traces also show that the 135 Å emission from the Li tracer is much brighter than that from the plastic shell [Fig. 6(b)].

III. DESIGN OF A LOW- k FLUCTUATION TELESCOPE FOR NSTX

The above results show that by using multilayer mirror telescopes it is possible to collect with good efficiency and spectral discrimination the soft x-ray photons emitted by low- Z impurities in tokamaks. Bright, beam excited $\Delta n=1$ lines such as H_α from intrinsic C, or Ly_α from Li pellets could then be used to image turbulent fluctuations deep in the NSTX core. In addition, our data suggest that $n=2-4$ transitions might also be of interest for fluctuation imaging.

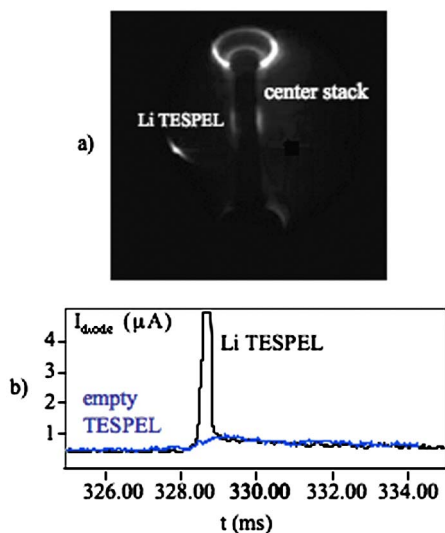


FIG. 6. (Color online) (a) Image in Li I light of Li filled TESPEL, injected in low density NSTX L mode. (b) Telescope traces following injection of empty and Li filled TESPEL pellets in low density L mode. A current amplifier with 10^6 V/A gain and no diode bias was used in this measurement.

Indeed, including collisional mixing, the CX emission cross section of the $n=2-4$ transition is about 1/4 that of the $n=2-3$ (H_α) transition.¹² Using then the beam excited C VI $n=2-3$ intensity in Fig. 1 as a reference, in H modes the beam excited C VI $n=2-4$ intensity would be $\geq 10^{14}$ photon/cm² sr s, i.e., about an order of magnitude higher than the above estimated C VI $n=2-4$ edge intensity (10^{13} photon/cm² sr s).

The low NSTX magnetic field also favors a BES-type fluctuation diagnostic. The thermal ion gyroradius is $\rho_i \approx 1-1.5$ cm, implying that spatial resolution of this order should be adequate for imaging fluctuation with poloidal wave number $k_\theta < 1/\rho_i$. A telescope field of view around 12×12 cm² would then enable correlating the long wavelength radial and poloidal fluctuations in NSTX.

The bandwidth requirements are also somewhat relaxed at low field. Making the usual assumption that the turbulent fluctuations are Doppler shifted by the plasma poloidal rotation to an effective frequency $v_{pol}k_\theta$, and assuming a poloidal wavelength of a few ρ_i , one obtains using the neoclassical computed poloidal rotation in NSTX, a fluctuation frequency range between several tens and a few hundred kilohertz.

Finally, the centimeter sized ion gyroradii in NSTX, together with the nearly flat central density profiles in H modes,¹³ suggest that relatively large amplitude density fluctuations may be present. Taking for instance the mixing-length estimate of the perturbation amplitude $\delta n/n \approx \lambda_\perp/L_n$ (Ref. 14) and assuming a perpendicular wavelength λ_\perp of the perturbation of a few ρ_i , with the central density scale length $L_n \approx 100$ cm, the estimated fluctuation amplitude is a few percent.

One difficulty with an imaging turbulence diagnostic for the NSTX core is the rapid variation of the field line pitch angle with major radius at a given time and with time at a given radius. Towards the plasma center, however, the H -mode q -profile tends to be flat, which reduces the extent of pitch angle variations. For instance, our calculations show that a telescope tilted at 10° with respect to the horizontal plane and viewing the region between 110 and 120 cm, would see only about a $\pm 2.5^\circ$ variation in pitch angle at a given instant and an overall variation of only a few degrees during the discharge evolution.

As an example of a fluctuation diagnostic we consider a 5 in. telescope at the C VI H_α wavelength, imaging with ≈ 5 demagnification a 12×12 cm² cross section of beam A, centered at $R \approx 115$ cm. Using a $R=0.75$ m Al/Zr spherical mirror of $2d \approx 190$ Å at $\theta_B=84^\circ$ (at longer wavelengths and normal incidence Al/Zr offers narrower band pass than Mo/Si), a Mo/Si planar mirror of $2d \approx 300$ Å at 45° incidence, and a $0.3 \mu\text{m}$ Be/ $0.1 \mu\text{m}$ Parylene-N visible light filter, the overall optical transmission is around 5%. Assuming then 2% carbon concentration in the beam volume and 2×5 mm² detector pixels, the H_α photon rate is 10^{11} photon s⁻¹ per pixel, corresponding to a statistical noise of 0.2% with $2 \mu\text{s}$ integration time. Using as detectors 2×5 mm AXUV-16 diode arrays,¹⁰ the detected current would be 500 nA. Our tests show that using optimized amplifiers and low capacitance AXUV diodes, SNR ≥ 200 and bandwidth ≥ 500 kHz are achievable at this signal level. Concerning plasma noise, the

large amplitude “spikes” from neutron and gamma interactions will have little effect on cross correlated fluctuation measurements and they can also be digitally eliminated, or the detector shielded from nuclear radiation. The “optical” soft x-ray array is another telescope detector we study, of particular interest for 2D fluctuation measurements.¹⁵

In conclusion, we assess that using MLM telescopes it would be possible to image turbulent fluctuations in the NSTX core having $\geq 0.5\%$ amplitude and \leq few hundred kilohertz frequency. Using localized impurity deposition from TESPEL pellets, the SXR telescope, and an impurity density diagnostic,⁵ it would also be possible to perform a simultaneous measurement of turbulence and local particle transport using the pellet SXR emission.

ACKNOWLEDGMENTS

The telescope mirrors were provided through a NIFS/JHU collaboration. The work at Johns Hopkins is supported by U.S. DOE through Grant No. DE-FG02-99ER54523. Any references to commercial products do not constitute endorsement by NIST or the U.S. Government.

- ¹R. J. Fonck, P. A. Duperrex, and S. F. Paul, *Rev. Sci. Instrum.* **61**, 3487 (1990).
- ²G. McKee, C. Fenzi, R. Fonck, and M. Jakubowski, *Rev. Sci. Instrum.* **74**, 2014 (2003).
- ³D. Stutman, M. Finkenthal, V. Soukhanovskii, M. J. May, H. W. Moos, and R. Kaita, *Rev. Sci. Instrum.* **72**, 732 (2001).
- ⁴N. Tamura *et al.*, *Plasma Phys. Controlled Fusion* **45**, 27 (2003).
- ⁵D. Stutman *et al.*, *Rev. Sci. Instrum.* **76**, 013508 (2005).
- ⁶R. J. Fonck, D. S. Darrow, and H. P. Jaehnig, *Phys. Rev. A* **29**, 3288 (1984).
- ⁷G. R. McKee, R. J. Fonck, C. Fenzi, and B. P. Leslie, *Rev. Sci. Instrum.* **72**, 992 (2001).
- ⁸<http://www.ntt-at.com>
- ⁹<http://www.lebowcompany.com/>
- ¹⁰<http://www.ird-inc.com/>
- ¹¹<http://www.accent.ro/>
- ¹²R. C. Isler, *Plasma Phys. Controlled Fusion* **36**, 171 (1994).
- ¹³S. Kaye *et al.*, *Nucl. Fusion* **45**, S168 (2005).
- ¹⁴J. Wesson, *Tokamaks*, 3rd ed. (Clarendon, Oxford, 2004), Chap. 4; L. F. Delgado-Aparicio, D. Stutman, K. Tritz, M. Finkenthal, R. Kaita, L. Roquemore, D. Johnson, and R. Majeski, *Rev. Sci. Instrum.* **75**, 4020 (2004).
- ¹⁵L. F. Delgado-Aparicio, D. Stutman, K. Tritz, M. Finkenthal, R. Kaita, L. Roquemore, D. Johnson, and R. Majeski, *Rev. Sci. Instrum.* **75**, 4020 (2004).